Astro Ltd.

LETTER

Statics and dynamics of a self-bound dipolar matter-wave droplet

View the article online for updates and enhancements.

Related content

- Stable and mobile excited two-dimensional dipolar Bose–Einstein condensate solitons
  S K Adhikari

- Stable and mobile two-dimensional dipolar ring-dark-in-bright Bose–Einstein condensate soliton
  S K Adhikari

- Two-dimensional bright and dark-in-bright dipolar Bose–Einstein condensate solitons on a one-dimensional optical lattice
  S K Adhikari

Recent citations

- Frontiers in multidimensional self-trapping of nonlinear fields and matter
  Yaroslav V. Kartashov *et al*

- Hydrodynamic model of a Bose–Einstein condensate with anisotropic short-range interaction and bright solitons in a repulsive Bose–Einstein condensate
  Pavel A Andreev

- Self-trapped quantum balls in binary Bose–Einstein condensates
  Sandeep Gautam and S K Adhikari

IOP ebooks™

Bringing you innovative digital publishing with leading voices to create your essential collection of books in STEM research.

Start exploring the collection - download the first chapter of every title for free.

Letter

Statics and dynamics of a self-bound dipolar matter-wave droplet

S K Adhikari[1]

Instituto de Física Teórica, UNESP—Universidade Estadual Paulista, 01.140-070 São Paulo, São Paulo, Brazil

E-mail: Adhikari@ift.unesp.br

CrossMark

Abstract

We study the statics and dynamics of a stable, mobile, *self-bound* three-dimensional dipolar matter-wave droplet created in the presence of a tiny repulsive three-body interaction. In frontal collision with an impact parameter and in angular collision at large velocities along all directions two droplets behave like quantum solitons. Such a collision is found to be quasi elastic and the droplets emerge undeformed after collision without any change of velocity. However, in a collision at small velocities the axisymmeric dipolar interaction plays a significant role and the collision dynamics is sensitive to the direction of motion. For an encounter along the z direction at small velocities, two droplets, polarized along the z direction, coalesce to form a larger droplet—a droplet molecule. For an encounter along the x direction at small velocities, the same droplets stay apart and never meet each other due to the dipolar repulsion. The present study is based on an analytic variational approximation and a numerical solution of the mean-field Gross–Pitaevskii equation using the parameters of ^{52}Cr atoms.

Keywords: Bose–Einstein condensate, Gross–Pitaevskii equation, soliton, dipolar atoms

(Some figures may appear in colour only in the online journal)

1. Introduction

After the observation of Bose–Einstein condensate (BEC) [1, 2] of alkali atoms, there have been many experimental studies to explore different quantum phenomena involving matter wave previously not accessible for investigation in a controlled environment, such as, quantum phase transition [3], vortex-lattice formation [4], collapse [5], four-wave mixing [6], interference [7], Josephson tunneling [8], Anderson localization [9] etc. The generation and the dynamics of self-bound quantum wave have drawn much attention lately [10]. There have been studies of self-bound matter waves or solitons in one (1D) [10] or two (2D) [11, 12] space dimensions. A soliton travels at a constant velocity in 1D, due to a cancellation of nonlinear attraction and defocusing forces [13]. The 1D soliton has been observed in a BEC [10]. However, a two- or three-dimensional (3D) soliton cannot be realized for two-body contact attraction alone due to collapse [13].

There have been a few proposals for creating a self-bound 2D and 3D matter-wave state which we term a droplet exploiting extra interactions usually neglected in a dilute BEC of alkali atoms [1]. In the presence of an axisymmetric nonlocal dipolar interaction [14] a 2D BEC soliton can be generated in a 1D harmonic [11] or a 1D optical-lattice [12] trap. Maucher *et al* [15] suggested that for Rydberg atoms, off-resonant dressing to Rydberg nD states can provide a nonlocal long-range attraction which can form a 3D matter-wave droplet. In this Letter we demonstrate that a tiny repulsive three-body interaction can avoid collapse and form a stable self-bound dipolar droplet in 3D [16]. There have been experimental [17]

[1] www.ift.unesp.br/users/Adhikari

and theoretical [18] studies of the formation of a trapped dipolar BEC droplet. In fact, for dipolar interaction stronger than two-body contact repulsion, a dipolar droplet has a net attraction [19, 20]; but the two-body contact repulsion is too weak to stop the collapse, whereas a three-body contact repulsion can eliminate the collapse and form a stable stationary droplet. Such a droplet can also be formed in a nondipolar BEC (details to be reported elsewhere) [21].

We study the frontal collision with an impact parameter and angular collision between two dipolar droplets. Only the collision between two integrable 1D solitons is truly elastic [10, 13]. As the dimensionality of the soliton is increased such collision is expected to become inelastic with loss of energy in 2D and 3D. In the present numerical simulation at large velocities all collisions are found to be quasi elastic while the droplets emerge after collision with practically no deformation and without any change of velocity.

Due to axisymmetric dipolar interaction, two droplets polarized along the z direction, attract each other when placed along the z axis and repel each other when placed along the x axis and the collision dynamics along x and z directions has different behaviors at very small velocities. For a collision between two droplets along the z direction, the two droplets form a single bound entity in an excited state, termed a 3D droplet molecule [22]. However, at very small velocities for an encounter along the x direction, the two droplets repel and stay away from each other due to dipolar repulsion and never meet.

The dipolar interaction potential, being not absolutely integrable, does not enjoy well defined Fourier transform that would appear for an infinite system [23]. Therefore, to get meaningful results, it is necessary either to regularize this potential, or, which is equivalent, to deal only with finite systems, where the system size plays the role of an effective regularization. That is, as soon as atomic interactions include dipolar forces, only finite systems are admissible. In other words, the occurrence of dipole forces prescribes the system to be finite, either being limited by an external trapping potential or forming a kind of a self-bound droplet. The conditions of stability of such droplets are studied in the present manuscript.

2. Mean-field model

The *trapless* mean-field Gross–Pitaevskii (GP) equation for a self-bound dipolar droplet of N atoms of mass m in the presence of a three-body repulsion is [2, 24]

$$
i\hbar \frac{\partial \phi(\mathbf{r}, t)}{\partial t} = \left[-\frac{\hbar^2}{2m}\nabla^2 + \frac{4\pi\hbar^2 aN}{m}|\phi|^2 + \frac{\hbar N^2 K_3}{2}|\phi|^4 \right.
$$
$$
\left. + 3a_{dd}N \int U_{dd}(\mathbf{R})|\phi(\mathbf{r}', t)|^2 d\mathbf{r}' \right] \phi(\mathbf{r}, t), \quad (1)
$$

$$
a_{dd} \equiv \frac{m\mu_0\mu_d^2}{12\pi\hbar^2}, \quad U_{dd}(\mathbf{R}) = \frac{1 - 3\cos^2\theta}{R^3}, \quad (2)
$$

where a is the scattering length, $\mathbf{R} = (\mathbf{r} - \mathbf{r}')$, θ is the angle between the vector $\mathbf{R}$ and the polarization direction z, μ_0 is the permeability of free space, μ_d is the magnetic dipole moment

of each atom, and K_3 is the three-body interaction term. This mean-field equation has recently been used by Blakie [24][2] to study a trapped dipolar BEC. We can obtain a dimensionless equation, by expressing length in units of a scale l and time in units of $\tau \equiv ml^2/\hbar$. Consequently, (1) can be rewritten as

$$
i\frac{\partial \phi(\mathbf{r}, t)}{\partial t} = \left[-\frac{\nabla^2}{2} + 4\pi aN|\phi|^2 + \frac{K_3N^2}{2}|\phi|^4 \right.
$$
$$
\left. + 3a_{dd}N \int U_{dd}(\mathbf{R})|\phi(\mathbf{r}', t)|^2 d\mathbf{r}' \right] \phi(\mathbf{r}, t), \quad (3)
$$

where K_3 is expressed in units of $\hbar l^4/m$ and $|\phi|^2$ in units of l^{-3} and energy in units of $\hbar^2/(ml^2)$. The wave function is normalized as $\int |\phi(\mathbf{r}, t)|^2 d\mathbf{r} = 1$.

For an analytic understanding of the formation of a droplet a variational approximation of (3) is obtained with the axisymmetric Gaussian ansatz: [25–27]

$$
\phi(\mathbf{r}) = \frac{\pi^{-3/4}}{w_z^{1/2}w_\rho} \exp\left[-\frac{\rho^2}{2w_\rho^2} - \frac{z^2}{2w_z^2} \right], \quad (4)
$$

where $\rho^2 = x^2 + y^2$, w_ρ and w_z are the radial and axial widths, respectively. This leads to the energy density per atom:

$$
\mathcal{E}(\mathbf{r}) = \frac{|\nabla\phi(\mathbf{r})|^2}{2} + 2\pi Na|\phi(\mathbf{r})|^4 + \frac{K_3N^2}{6}|\phi(\mathbf{r})|^6
$$
$$
+ \frac{3a_{dd}N}{2}|\phi(\mathbf{r})|^2 \int U_{dd}(\mathbf{R})|\phi(\mathbf{r}')|^2 d\mathbf{r}', \quad (5)
$$

and the total energy per atom $E \equiv \int \mathcal{E}(\mathbf{r})d\mathbf{r}$ [26]:

$$
E = \frac{1}{2w_\rho^2} + \frac{1}{4w_z^2} + \frac{K_3N^2\pi^{-3}}{18\sqrt{3}\, w_\rho^4 w_z^2} + \frac{N[a - a_{dd}f(\kappa)]}{\sqrt{2\pi}\, w_\rho^2 w_z}, \quad \kappa = w_\rho/w_z,
$$
$$
(6)
$$

$$
f(\kappa) = \frac{1 + 2\kappa^2 - 3\kappa^2 d(\kappa)}{1 - \kappa^2}, \quad d(\kappa) = \frac{\text{atanh}\sqrt{1 - \kappa^2}}{\sqrt{1 - \kappa^2}}. \quad (7)
$$

In (6), the first two terms on the right are contributions of the kinetic energy of the atoms, the third term on the right corresponds to the three-body repulsion, and the last term to the net attractive atomic interactions responsible for the formation of the droplet for $|a| > a_{dd}$. The higher order nonlinearity (quintic) of the three-body interaction compared to the cubic nonlinearity of the two-body interaction, has led to a more singular repulsive term at the origin in (6). This makes the system highly repulsive at the center ($w_\rho, w_z \to 0$), even for a small three-body repulsion, and stops the collapse stabilizing the droplet.

The stationary widths w_ρ and w_z of a droplet correspond to the global minimum of energy (6) [26, 27]

$$
\frac{1}{w_\rho^3} + \frac{N}{\sqrt{2\pi}}\frac{[2a - a_{dd}g(\kappa)]}{w_\rho^3 w_z} + \frac{4K_3N^2}{18\sqrt{3}\,\pi^3 w_\rho^5 w_z^2} = 0, \quad (8)
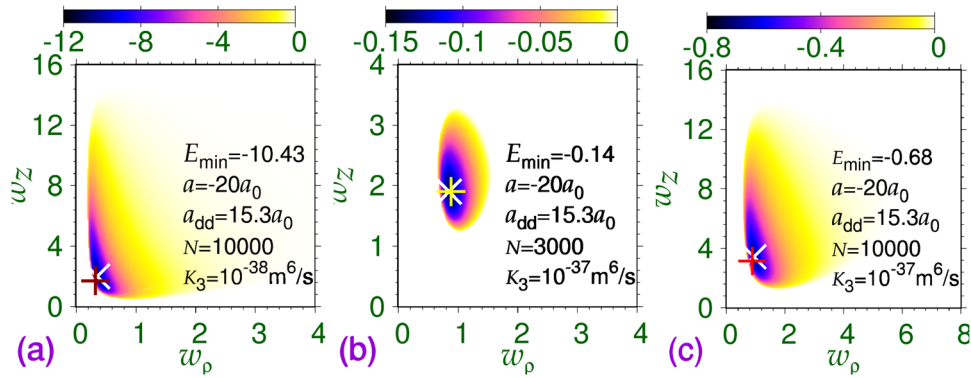$$

Figure 1. 2D contour plot of energy (6) showing the energy minimum and the negative energy region for ^{52}Cr atoms as a function of widths w_ρ and w_z for (a) $N = 10\,000$, $K_3 = 10^{-38}$ m^6 s^{-1}, (b) $N = 3000$, $K_3 = 10^{-37}$ m^6 s^{-1} and (c) $N = 10\,000$, $K_3 = 10^{-37}$ m^6 s^{-1}. The variational and numerical widths of the stationary droplet are marked $\times$ and $+$, respectively. Plotted quantities is all figures are dimensionless and the physical unit for ^{52}Cr atoms can be restored using the unit of length $l = 1$ μm.
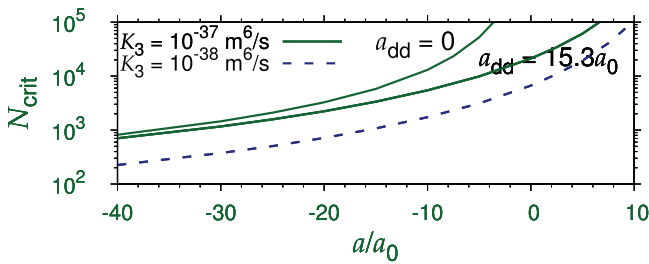

Figure 2. Variational critical number of atom N_{crit} for the formation of dipolar ($a_{dd} = 15.3a_0$) and nondipolar ($a_{dd} = 0$) droplets, obtained from (8) and (9), for different K_3. For $N < N_{crit}$ and for $a > a_{dd} = 15.3a_0$ (dipolar) and for $a > 0$ (nondipolar) no droplet can be formed.

$$\frac{1}{w_z^3} + \frac{2N}{\sqrt{2\pi}} \frac{[a - a_{dd}c(\kappa)]}{w_\rho^2 w_z^2} + \frac{4K_3N^2}{18\sqrt{3}\,\pi^3 w_\rho^4 w_z^3} = 0, \quad (9)$$

$$g(\kappa) = \frac{2 - 7\kappa^2 - 4\kappa^4 + 9\kappa^4 d(\kappa)}{(1 - \kappa^2)^2},$$

$$c(\kappa) = \frac{1 + 10\kappa^2 - 2\kappa^4 - 9\kappa^2 d(\kappa)}{(1 - \kappa^2)^2}.$$

3. Numerical results

Unlike the 1D case, the 3D GP equation (3) does not have an analytic solution and different numerical methods, such as split-step Crank–Nicolson [28] and Fourier spectral [29] methods, are used for its solution. We solve the 3D GP equation (3) numerically by the split-step Crank–Nicolson method [28] for a dipolar BEC [27, 30] using both real- and imaginary-time propagation in Cartesian coordinates employing a space step of 0.025 and a time step upto as small as 0.000 01. In numerical calculation, we use the parameters of ^{52}Cr atoms [26], e.g. $a_{dd} = 15.3a_0$ and $m = 52$ amu with a_0 the Bohr radius. We take the unit of length $l = 1$ μm, unit of time $\tau \equiv ml^2/\hbar = 0.82$ ms and the unit of energy $\hbar^2/(ml^2) = 1.29 \times 10^{-31}$ J.

The scattering length a can be controlled experimentally, independent of the three-body term K_3, by magnetic [31]

and optical [32] Feshbach resonances and we mostly fix $a = -20a_0$ below. In figures 1 we show the 2D contour plot of energy (6) as a function of widths w_ρ and w_z for different N and K_3. This figure highlights the negative energy region. The white region in this plot corresponds to positive energy. The minimum of energy is clearly marked in figures 1.

For a fixed scattering length a, (8) and (9) for variational widths allow solution for the number of atoms N greater than a critical value N_{crit}. For $N < N_{crit}$ the system is much too repulsive and escapes to infinity. However, this critical value N_{crit} of N is a function of the three-body term K_3 and scattering length a. The $N_{crit} - a$ correlation for different K_3 is shown in figure 2. The critical number of atoms for the formation of a nondipolar droplet for $K_3 = 10^{-37}$ m^6 s^{-1} is also shown in this figure. Although a trapped dipolar BEC with a negligible K_3 collapses for a sufficiently large N [33], there is no collapse of the droplets for a large N due to a very strong three-body repulsion at the center.

We compare in figure 3(a) the numerical and variational root-mean-square (rms) sizes ρ_{rms} and z_{rms} of a droplet versus N for two different K_3: 10^{-38} m^6 s^{-1}, and 10^{-37} m^6 s^{-1}. These values of K_3 are reasonable and are similar to the values of K_3 used elsewhere [24, 34]. In figure 3(b) we show the numerical and variational energies $|E|$ of a droplet versus N for different K_3. The energy of a bound droplet is negative in all cases and its absolute value is plotted.

To study the density distribution of a ^{52}Cr droplet we calculate the reduced 1D densities $\rho_{1D}(x) \equiv \int dz dy |\phi(\mathbf{r})|^2$, and $\rho_{1D}(z) \equiv \int dx dy |\phi(\mathbf{r})|^2$. In figure 4 we plot these densities as obtained from variational and numerical calculations for different N and K_3. From figures 3(a) and 4(a)–(d) we find that for a small N and fixed K_3, the droplets are well localized with small size and the agreement between numerical and variational results is better. For a fixed N, the droplet is more compact for a small K_3 corresponding to a small three-body repulsion.

In figures 5(a)–(d) we show the 3D isodensity contours of the droplets of figures 4(a)–(d), respectively. In all cases the droplets are elongated in the z direction due to dipolar interaction. In figures 5(a)–(b) and 4(a)–(b) K_3 is much larger than that in figures 5(c)–(d) and 4(c)–(d). Hence, the three-body repulsion is stronger in figures 5(a)–(b) thus leading to
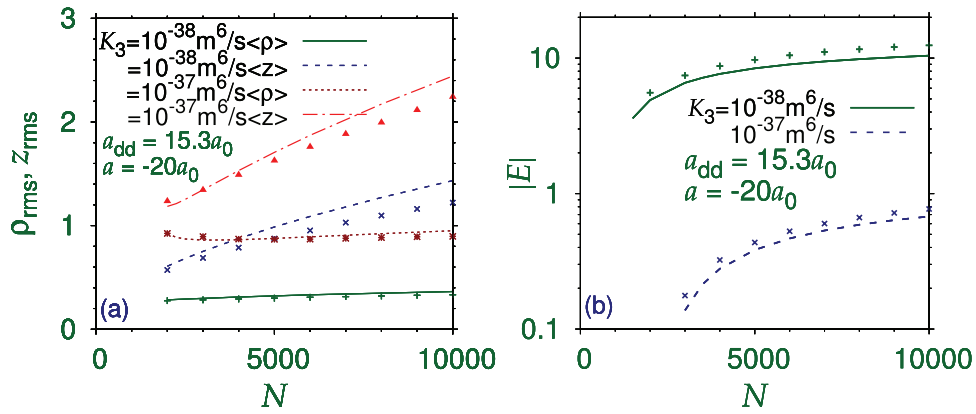
Figure 3. Variational (line) and numerical (chain of symbols) (a) rms sizes ρ_{rms}, z_{rms} and (b) energy $|E|$ versus the number of ^{52}Cr atoms N in a droplet for two different K_3: 10^{-38} m^6 s^{-1} and 10^{-37} m^6 s^{-1}. The physical unit of energy for ^{52}Cr atoms can be restored by using the energy scale 1.29×10^{-31} J.
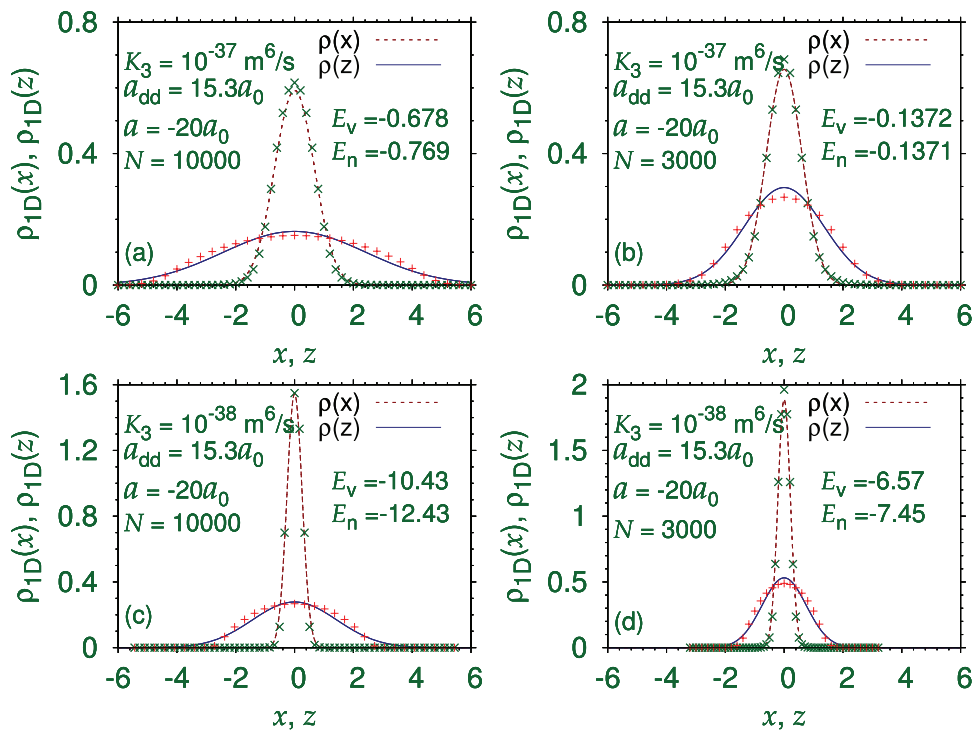

Figure 4. Variational (v, line) and numerical (n, chain of symbols) reduced 1D densities $\rho_{1D}(x)$ and $\rho_{1D}(z)$ along x and z directions, respectively, and corresponding energies of a ^{52}Cr droplet with $a = -20a_0$ for different N and K_3: (a) $N = 10\,000$, $K_3 = 10^{-37}$ m^6 s^{-1}, (b) $N = 3000$, $K_3 = 10^{-37}$ m^6 s^{-1}, (c) $N = 10\,000$, $K_3 = 10^{-38}$ m^6 s^{-1}, and (d) $N = 3000$, $K_3 = 10^{-38}$ m^6 s^{-1}.

droplets of larger sizes. In contrast to a local energy minimum in 1D [10] and 2D [11] solitons, the 3D droplets correspond to a global energy minimum with $E < 0$, viz figures 1, and are expected to be stable. The stability of the droplets is confirmed (details to be reported elsewhere) by real-time simulation over a long time interval upon a small perturbation. and extreme inelastic collision with the formation of droplet molecule is possible for $v < 1$.

To test the solitonic nature of the droplets, we study the frontal head-on collision and collision with an impact parameter d of two droplets at large velocity along x and z axes. To set the droplets in motion the respective imaginary-time wave functions are multiplied by $\exp(\pm i\nu x)$ and real-time simulation is then performed with these wave functions. Due to the

axisymmetric dipolar interaction the dynamics along x and z axes could be different at small velocities. At large velocities the kinetic energy E_k of the droplets is much larger than the internal energies of the droplets, and the latter plays an insignificant role in the collision dynamics. Consequently, there is no qualitative difference between the collision dynamics along x and z axes and that between the collision dynamics for different impact parameters at large velocities. As velocity is reduced, the collision becomes inelastic resulting in a deformation and eventual destruction of the individual droplets after collision. At very small velocities, the dipolar energy plays a decisive role in collision along x and z axes, and the dynamics along these two axes have completely different characteristics, viz figure 9.
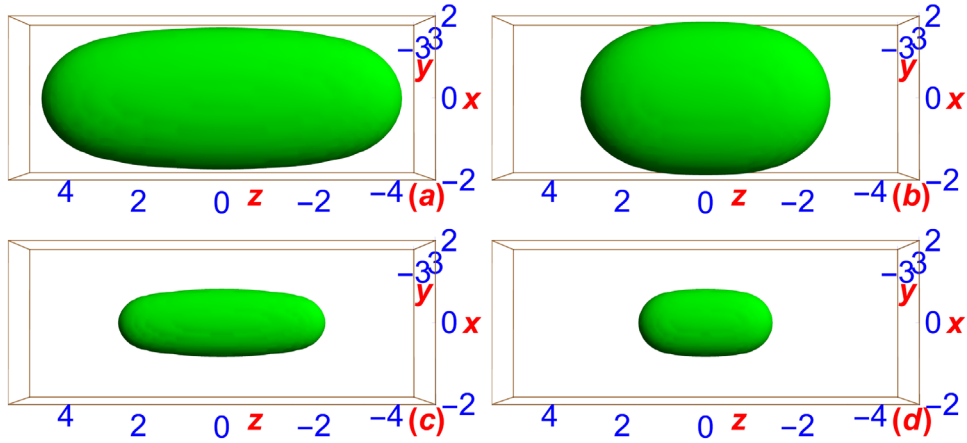
Figure 5. The 3D isodensity $(|\phi(\mathbf{r})|^2)$ of the droplets of (a) figures 4(a)–(d) (b). The dimensionless density on the contour in figures 5 and 6–8 is 0.001 which transformed to physical units is 10^9 atoms cc^{-1}.
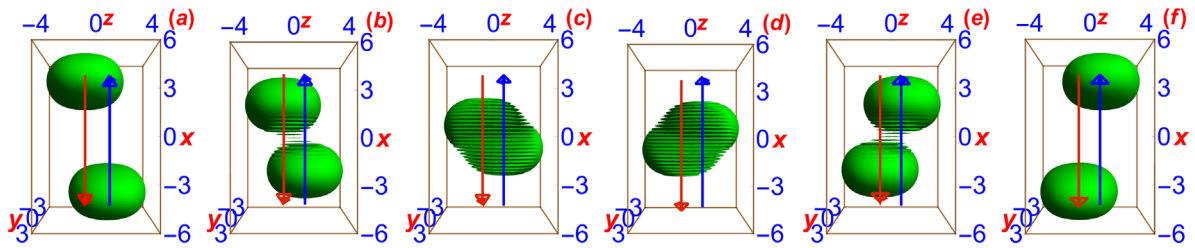

Figure 6. Collision dynamics of two droplets of figure 4(b) placed at $x = \pm 4, z = \mp 1$ at $t = 0$ moving in opposite directions along the x axis with velocity $v \approx 38$, illustrated by 3D isodensity contours at times (a) $t = 0$, (b) $= 0.042$, (c) $= 0.084$, (d) $= 0.126$, (e) $= 0.168$, (f) $= 0.210$. The velocities of the droplets are shown by arrows.
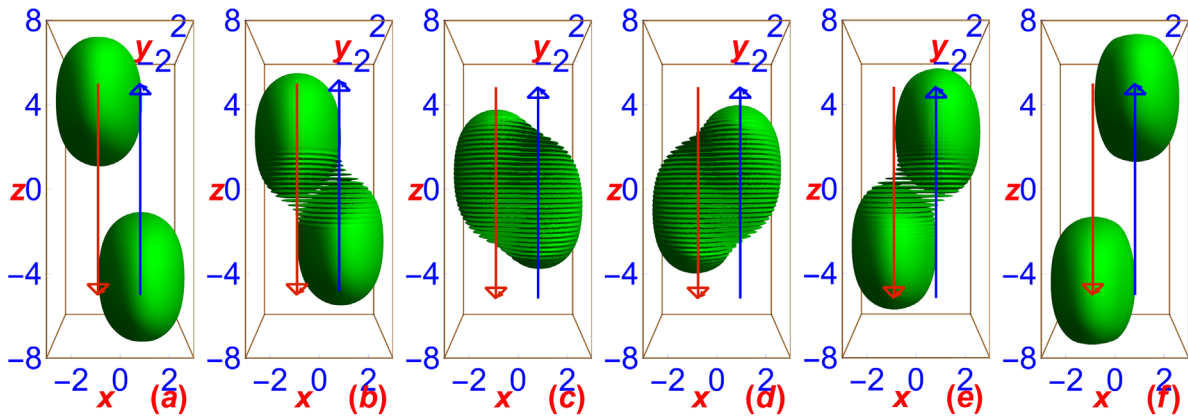

Figure 7. Collision dynamics of two droplets of figure 4(b) placed at $x = \pm 1, z = \mp 4.8$ at $t = 0$ moving in opposite directions along the z axis with velocity $v \approx 37$ by 3D isodensity contours at times (a) $t = 0$, (b) $= 0.052$, (c) $= 0.104$, (d) $= 0.156$, (e) $= 0.208$, (f) $= 0.260$.

The collision dynamics of two droplets of figure 4(b) ($N = 3000, K_3 = 10^{-37}$ m^6 s^{-1}) moving along the x axis in opposite directions with a velocity $v \approx 38$ each and with an impact parameter $d = 2$ is shown in figures 6(a)–(f) by successive snapshots of 3D isodensity contour of the moving droplets. A similar collision dynamics of the same droplets moving along the z axis with a velocity $v \approx 37$ each with impact parameter $d = 2$ is illustrated in figures 7(a)–(f). The droplets come close to each other in figures 6(b) and 7(b), coalesce to form a single entity in figures 6(c)–(d) and 7(c)–(d), form two separate droplets in figures 6(e) and 7(e). The droplets are well separated in figures 6(f) and 7(f) without visible

deformation/distortion in shape and moving along x and z axes with the same initial velocity showing the quasi elastic nature of collision. The frontal head-on collision is also quasi elastic.

To study the angular collision of two droplets of figure 4(b), at $t = 0$ two droplets of are placed at $x = \pm 3, z = 1$, respectively, and set into motion towards the origin with a velocity $v \approx 40$ each by multiplying the respective imaginary-time wave functions by $\exp(\pm i50x + 9.5iz)$ and performing real-time simulation. Again the isodensity profiles of the droplets before, during, and after collision are shown in figures 8(a)–(b), (c)–(d) and (e)–(f), respectively. The droplets again come out after collision undeformed conserving their velocities.
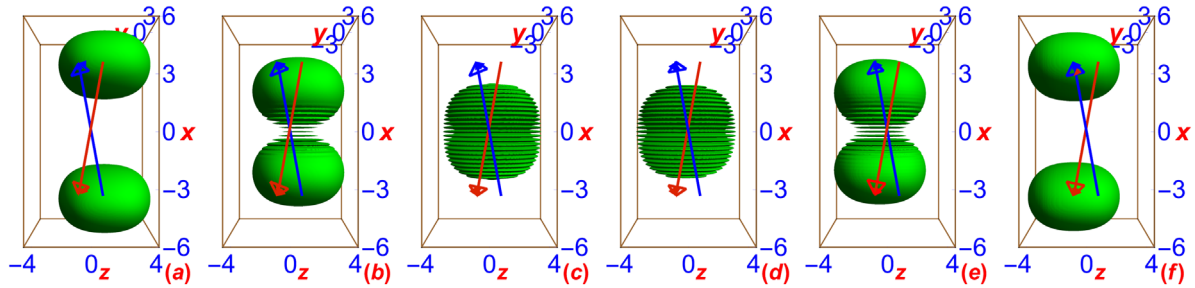
Figure 8. Collision dynamics of two droplets of figure 4(b) placed at $x = \pm 4$, $z = 1$ at $t = 0$ moving towards origin with velocity $v \approx 40$ by 3D isodensity plots at times (a) $t = 0$, (b) $= 0.042$, (c) $= 0.084$, (d) $= 0.126$, (e) $= 0.168$, (f) $= 0.210$.

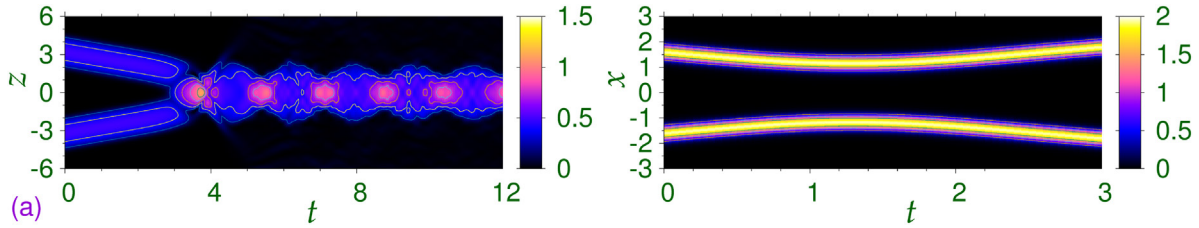**Figure 9.** (a) 2D contour plot of the evolution of 1D density $\rho_{1D}(z, t)$ versus z and t during the collision of two droplets of figure 4(d) initially placed at $z = \pm 3.2$ at $t = 0$ and moving towards each other with velocity $v \approx 0.5$. (b) 2D contour plot of the evolution of 1D density $\rho_{1D}(x, t)$ versus x and t during the encounter of the same droplets initially placed at $x = \pm 1.6$ at $t = 0$ and moving towards each other with velocity $v \approx 0.5$.

Two dipolar droplets placed along the x axis with the dipole moment along the z directions repel by the long range dipolar interaction, whereas the two placed along the z axis attract each other by the dipolar interaction. This creates a dipolar barrier between the two colliding droplets along the x direction. At large incident kinetic energies, the droplets can penetrate this barrier and collide along the x direction. However, at very small kinetic energies ($v < 1$), for an encounter along the x direction the droplets cannot overcome the dipolar barrier and the collision does not take place. There is no such barrier for an encounter along the z direction at very small velocities and the encounter takes place with the formation of a oscillating droplet molecule. To illustrate the different nature of the dynamics of collision along x and z directions at very small velocities we consider two droplets of figure 4(d) ($N = 3000$; $K_3 = 10^{-38}$ m^6 s^{-1}). For an encounter along the z direction at $t = 0$ two droplets are placed at $z = \pm 3.2$ and set in motion in opposite directions along the z axis with a small velocity $v \approx 0.5$. The dynamics is illustrated by a 2D contour plot of the time evolution of the 1D density $\rho_{1D}(z, t)$ in figure 9(a). The two droplets come close to each other at $z = 0$ and coalesce to form a droplet molecule and never separate again. The droplet molecule is formed in an excited state due to the liberation of binding energy and hence oscillates. For an encounter along the x direction at $t = 0$ two droplets are placed at $x = \pm 1.6$ and set in motion in opposite directions along the x axis with the same velocity $v \approx 0.5$. The dynamics is illustrated by a 2D contour plot of the time evolution of the 1D density $\rho_{1D}(x, t)$ in figure 9(b). The droplets come a little closer to each other due to the initial momentum. But due to long-range dipolar repulsion they move away from each other eventually and the actual encounter never takes place. In collision dynamics of nondipolar BECs and in collision

of dipolar BEC along z direction the BECs never exhibit this peculiar behavior.

A semi-quantitative estimate of the dipolar repulsion of the collision of two droplets along the x axis at small velocities can be given by the variational expression for energy per atom (6) for a fixed w_z, e.g.

$$E(w_\rho) = \frac{1}{2w_\rho^2} + \frac{K_3 N^2 \pi^{-3}}{18\sqrt{3}\, w_\rho^4 w_z^2} + \frac{N[a - a_{dd}f(\kappa)]}{\sqrt{2\pi}\, w_\rho^2 w_z}, \quad (10)$$

where we have removed the w_z-dependent constant term. Equation (10) gives the energy well felt by an individual atom approaching the droplet along the x axis. The single approaching atom will interact with all atoms of the droplet distributed along the extention of the droplet along the z direction (~ 0.8, viz figure 4(d)). The most probable z value of an atom in the droplet to interact with the approaching atom is $z_{rms} \sim w_z/\sqrt{2} \approx 0.5$. In figure 10 we plot $E(w_\rho)$ versus w_ρ with the parameters of the droplet of figure 4(d) employed in the dynamics shown in figure 9. We find in this figure that for small w_z the energy well is entirely repulsive. For medium values of w_z an attractive well with a repulsive dipolar barrier appears and for large w_z a fully attractive well appears without the dipolar barrier, which is also the case of an approaching atom along the z axis. For the probable w_z values there is a dipolar energy barrier of height ~ 0.2 near $w_\rho \sim 2$ to 3. For the dynamics in figure 9, the approaching atom has an energy of $v^2/2 = 0.5^2/2 = 0.125$, which is smaller than the height of the dipolar barrier at $w_\rho \sim 2$ to 3. Hence the approaching dipolar droplet in figure 9(b) turns back when the distance between the two droplets is ~ 2. In the collision along z direction there is no dipolar barrier and the encounter takes place at all velocities.
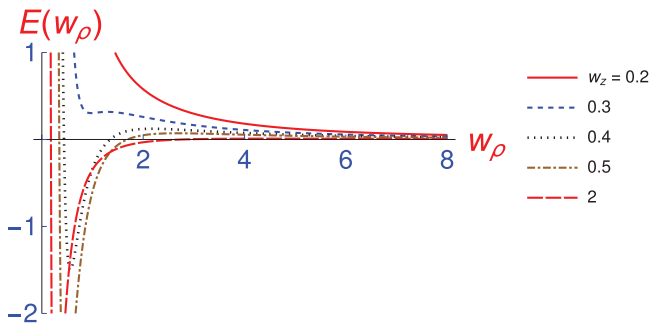
Figure 10. Energy well of (10) $E(w_\rho)$ versus w_ρ for different w_z with the parameters of the droplet of figure 4(d).

4. Summary

We demonstrated the creation of a stable, stationary self-bound dipolar BEC droplet for a tiny repulsive three-body contact interaction for $a_{dd} < |a|$ and study its statics and dynamics employing a variational approximation and numerical solution of the 3D GP equation (1). The droplet can move with a constant velocity. At large velocities, the frontal collision with an impact parameter and the angular collision of two droplets are found to be quasi elastic. At medium velocities, the collision is inelastic and leads to a deformation or a destruction of the droplets after collision. At very small velocities, the collision dynamics is sensitive to the anisotropic dipolar interaction and hence to the direction of motion of the droplets. The collision between two droplets along the z direction leads to the formation of a droplet molecule after collision. In an encounter along the x direction at very small velocities, the two droplets repel and stay away from each other avoiding a collision.

It seems appropriate to present a classification of the droplet formation in different parameter domains, e.g. scattering length a, dipolar length a_{dd}, the strength of three-body interactions K_3, and the number of atoms N. In the absence of dipolar interaction ($a_{dd} = 0$), a droplet can be formed for attractive atomic interaction ($a < 0$). In all cases there is a minimum number of atoms N_{crit} for the droplet formation, which increases as the three-body interaction K_3 increases or the scattering length a increases corresponds to less attraction, viz figure 2. There is no upper limit for the number of atoms to form a droplet. A similar panorama exists for the formation of a dipolar droplet with the exception that the dipolar droplet can be formed for $a < a_{dd}$.

The subject matter of this study is within present experimental possibilities as is clear from the stability plot of figure 2. The size of a trapped dipolar BEC is determined by the harmonic oscillator lengths of the trap, whereas the size of the present droplet is determined by the internal atomic interactions. One should start with a tapped dipolar BEC for $N < N_{crit}$ where no droplet can be formed, viz figure 2. Now using the Feshbach resonance technique, one should make the scattering length a more attractive to enter the droplet formation domain. If the harmonic trap is weak then initial droplet size could be relatively large, and by varying the scattering length the size of the droplet could be made much smaller

and such droplets have been detected in experiment [17]. The repulsive three-body force could be responsible for the formation of such droplets. Preliminary study has shown that such droplets can also be formed in nondipolar BECs in the presence of a repulsive three-body interaction [21].

References

[1] Anderson M H, Ensher J R, Matthews M R, Wieman C E and Cornell E A 1995 *Science* **269** 198
Davis K B, Mewes M O, Andrews M R, vanDruten N J, Durfee D S, Kurn D M and Ketterle W 1995 *Phys. Rev. Lett.* **75** 3969
Bradley C C, Sackett C A, Tollett J J and Hulet R G 1995 *Phys. Rev. Lett.* **75** 1687
[2] Dalfovo F, Giorgini S, Pitaevskii L P and Stringari S 1999 *Rev. Mod. Phys.* **71** 463
[3] Greiner M, Mandel O, Esslinger T, Hänsch T W and Bloch I 2002 *Nature* **415** 39
[4] Abo-Shaeer J R, Raman C, Vogels J M and Ketterle W 2001 *Science* **292** 476
[5] Donley E A, Claussen N R, Cornish S L, Roberts J L, Cornell E A and Wieman C E 2001 *Nature* **412** 295
Adhikari S K 2002 *Phys. Rev.* A **66** 013611
[6] Deng L, Hagley E W, Wen J, Trippenbach M, Band Y, Julienne P S, Simsarian J E, Helmerson K, Rolston S L and Phillips W D 1999 *Nature* **398** 218
[7] Andrews M R, Townsend C G, Miesner H-J, Durfee D S, Kurn D M and Ketterle W 1997 *Science* **275** 637
[8] Josephson B D 1962 *Phys. Lett.* **1** 251
Cataliotti F S, Burger S, Fort C, Maddaloni P, Minardi F, Trombettoni A, Smerzi A and Inguscio M 2001 *Science* **293** 843
Adhikari S K 2005 *Phys. Rev.* A **72** 013619
Adhikari S K 2003 *Eur. Phys. J.* D **25** 161
[9] Anderson P W 1958 *Phys. Rev.* **109** 1492
Billy J, Josse V, Zuo Z, Bernard A, Hambrecht B, Lugan P, Clément D, Sanchez-Palencia L, Bouyer P and Aspect A 2008 *Nature* **453** 891
Roati G, D'Errico C, Fallani L, Fattori M, Fort C, Zaccanti M, Modugno G, Modugno M and Inguscio M 2008 *Nature* **453** 895
Adhikari S K and Salasnich L 2009 *Phys. Rev.* A **80** 023606
[10] Pérez-Garcia V M, Michinel H and Herrero H 1998 *Phys. Rev.* A **57** 3837
Abdullaev F K, Gammal A, Kamchatnov A M and Tomio L 2005 *Int. J. Mod. Phys.* B **19** 3415
Strecker K E, Partridge G B, Truscott A G and Hulet R G 2002 *Nature* **417** 150
Khaykovich L, Schreck F, Ferrari G, Bourdel T, Cubizolles J, Carr L D, Castin Y and Salomon C 2002 *Science* **256** 1290
Nguyen J H V, Dyke P, Luo D, Malomed B A and Hulet R G 2014 *Nat. Phys.* **10** 918
[11] Pedri P and Santos L 2005 *Phys. Rev. Lett.* **95** 200404
Tikhonenkov I I, Malomed B A and Vardi A 2008 *Phys. Rev. Lett.* **100** 090406

Köberle P, Zajec D, Wunner G and Malomed B A 2012 *Phys. Rev.* A **85** 023630

Nath R, Pedri P and Santos L 2009 *Phys. Rev. Lett.* **102** 050401

[12] Adhikari S K 2016 *Laser. Phys. Lett.* **13** 085501

Adhikari S K and Muruganandam P 2012 *J. Phys. B: At. Mol. Phys.* **45** 045301

[13] Kivshar Y S and Malomed B A 1989 *Rev. Mod. Phys.* **61** 763

[14] Lu M, Burdick N Q, Youn S H and Lev B L 2011 *Phys. Rev. Lett.* **107** 190401

Aikawa K, Frisch A, Mark M, Baier S, Rietzler A, Grimm R and Ferlaino F 2012 *Phys. Rev. Lett.* **108** 210401

Lahaye T, Koch T, Fröhlich B, Fattori M, Metz J, Griesmaier A, Giovanazzi S and Pfau T 2007 *Nature* **448** 672

[15] Maucher F, Henkel N, Saffman M, Krlikowski W, Skupin S and Pohl T 2011 *Phys. Rev. Lett.* **106** 170401

[16] Bulgac A 2002 *Phys. Rev. Lett.* **89** 050402

[17] Kadau H, Schmitt M, Wenzel M, Wink C, Maier T, Ferrier-Barbut I and Pfau T 2016 *Nature* **530** 194

Schmitt M, Wenzel M, Bottcher F, Ferrier-Barbut I and Pfau T 2016 *Nature* **539** 259

[18] Xi K and Saito H 2016 *Phys. Rev.* A **93** 011604

[19] Lima A R P and Pelster A 2011 *Phys. Rev.* A **84** 041604

Lima A R P and Pelster A 2012 *Phys. Rev.* A **86** 063609

[20] Nikolic B, Balaž A and Pelster A 2013 *Phys. Rev.* A **89** 013624

Vidanovic I, Balaž A, Al-Jibbouri H and Pelster A *Phys. Rev.* A **84** 013618

[21] Adhikari S K unpublished

[22] Young S L E, Muruganandam P and Adhikari S K 2011 *J. Phys. B: At. Mol. Phys.* **44** 101001

Lakomy K, Nath R and Santos L 2012 *Phys. Rev.* A **86** 013610

[23] Yukalov V I and Yukalova E P 2016 *Laser Phys.* **26** 045501

[24] Blakie P B 2016 *Phys. Rev.* A **93** 033644

[25] Pérez-Garcia V M, Michinel H, Cirac J I, Lewenstein M and Zoller P 1996 *Phys. Rev. Lett.* **77** 5320

[26] Koch T, Lahaye T, Metz J, Frhlich B, Griesmaier A and Pfau T 2008 *Nat. Phys.* **4** 213

[27] Kumar R K, Young S L E, Vudragović D, Balaž A, Muruganandam P and Adhikari S K 2015 *Comput. Phys. Commun.* **195** 117

[28] Muruganandam P and Adhikari S K 2009 *Comput. Phys. Commun.* **180** 1888

Vudragović D, Vidanović I, Balaž A, Muruganandam P and Adhikari S K 2012 *Comput. Phys. Commun.* **183** 2021

Young S L E, Vudragović D, Muruganandam P, Adhikari S K and Balaž A 2016 *Comput. Phys. Commun.* **204** 209

Satarić B, Slavnić V, Belić A, Balaž A, Muruganandam P and Adhikari S K 2016 *Comput. Phys. Commun.* **200** 411

Lončar V, Young S L E, Škrbić S, Muruganandam P, Adhikari S K and Balaž A 2016 *Comput. Phys.* C **209** 190

[29] Muruganandam P and Adhikari S K 2003 *J. Phys. B: At. Mol. Opt. Phys.* **36** 2501

[30] Lončar V, Balaž A, Bogojević A, Skrbić S, Muruganandam P and Adhikari S K 2016 *Comput. Phys. Commun.* **200** 406

[31] Inouye S, Andrews M R, Stenger J, Miesner H-J, Stamper-Kurn D M and Ketterle W 1998 *Nature* **392** 151

Chin C, Julienne P and Tiesinga E 2010 *Rev. Mod. Phys.* **82** 1225

[32] Fatemi F K, Jones K M and Lett P D 2000 *Phys. Rev. Lett.* **85** 4462

[33] Ronen S, Bortolotti D C E and Bohn J L 2007 *Phys. Rev. Lett.* **98** 030406

Parker N G, Ticknor C, Martin A M and O'Dell D H J 2009 *Phys. Rev.* A **79** 013617

Ticknor C, Parker N G, Melatos A, Cornish S L, O'Dell D H J and Martin A M 2008 *Phys. Rev.* A **78** 061607

[34] Altin P A, Dennis G R, McDonald G D, Doring D, Debs J E, Close J D, Savage C M and Robins N P 2011 *Phys. Rev.* A **84** 033632